
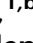









The interactive effects of temperature and nutrients on a spring phytoplankton community

Stephanie I. Anderson ^{1*,a} Gayantonia Franzè ^{1,b} Joshua D. Kling ^{2,c} Paul Wilburn ^{3,d}
Colin T. Kremer ⁴ Susanne Menden-Deuer ¹ Elena Litchman ³ David A. Hutchins ²
Tatiana A. Rynearson ^{1*}

¹Graduate School of Oceanography, University of Rhode Island, Narragansett, Rhode Island

²Department of Biological Sciences, University of Southern California, Los Angeles, California

³Michigan State University, Kellogg Biological Station, Hickory Corners, Michigan

⁴Department of Ecology and Evolutionary Biology, University of California Los Angeles, Los Angeles, California

Abstract

A complex interplay of environmental variables impacts phytoplankton community composition and physiology. Temperature and nutrient availability are two principal factors driving phytoplankton growth and composition, but are often investigated independently and on individual species in the laboratory. To assess the individual and interactive effects of temperature and nutrient concentration on phytoplankton community composition and physiology, we altered both the thermal and nutrient conditions of a cold-adapted spring phytoplankton community in Narragansett Bay, Rhode Island, when surface temperature was 2.6°C and chlorophyll > 9 $\mu\text{g L}^{-1}$. Water was incubated in triplicate at −0.5°C, 2.6°C, and 6°C for 10 d. At each temperature, treatments included both nutrient amendments (N, P, Si addition) and controls (no macronutrients added). The interactive effects of temperature and resource availability altered phytoplankton growth and community structure. Nutrient amendments resulted in species sorting and communities dominated by larger species. Under replete nutrients, warming tripled phytoplankton growth rates, but under in situ nutrient conditions, increased temperature acted antagonistically, reducing growth rates by as much as 33%, suggesting communities became nutrient limited. The temperature–nutrient interplay shifted the relative proportions of each species within the phytoplankton community, resulting in more silica rich cells at decreasing temperatures, irrespective of nutrients, and C : N that varied based on resource availability, with nutrient limitation inducing a 47% increase in C : N at increasing temperatures. Our results illustrate how the temperature–nutrient interplay can alter phytoplankton community dynamics, with changes in temperature amplifying or exacerbating the nutrient effect with implications for higher trophic levels and carbon flux.

Understanding biodiversity and its regulating factors is central to the study of ecology. In the phytoplankton, where an unexpectedly diverse group of organisms can coexist despite

possessing similar cellular requirements (Hutchinson 1961), deciphering the factors responsible for driving community composition is especially challenging. According to community assembly theory, species are funneled through a series of ordered filters which act on their respective traits to determine species composition (Keddy 1992; Pearson et al. 2018). The importance of each filter can be discerned through an evaluation of the species response, in terms of their relative abundance in the community (Pearson et al. 2018).

Two of the most important abiotic filters, or drivers, are temperature (Sunagawa et al. 2015) and nutrients (Redfield 1958). In phytoplankton, temperature can regulate growth and cellular metabolism (Eppeley 1972), while nutrients impact biomass by providing the elements needed to build cellular structures (Sterner and Elser 2002) and enhance enzymatically catalyzed pathways, like photosynthesis (Morel and Price 2003). Both factors influence microbial growth rates (Aranguren-Gassis et al. 2019; Boyd 2019) and may act as

*Correspondence: ryneerson@uri.edu, siander@mit.edu

This is an open access article under the terms of the Creative Commons Attribution-NonCommercial License, which permits use, distribution and reproduction in any medium, provided the original work is properly cited and is not used for commercial purposes.

Additional Supporting Information may be found in the online version of this article.

^aPresent address: Department of Earth, Atmospheric, and Planetary Sciences, Massachusetts Institute of Technology, Cambridge, Massachusetts

^bPresent address: Institute of Marine Research, Flødevigen Research Station, His, Norway

^cPresent address: Department of Plant and Microbiology, University of California, Berkeley, California

^dPresent address: NASA Ames Research Center, Mountain View, California

selective pressures on community diversity, with nutrient concentrations often shaping size distribution (Litchman et al. 2010) and temperature often driving species succession (Anderson and Rynearson 2020). Through passive transport along ocean currents, as well as seasonal cycles, phytoplankton are readily exposed to a variety of thermal conditions (Doblin and van Sebille 2016) and nutrient concentrations (Moore et al. 2013). Despite the complex conditions experienced in the natural environment, the effects of temperature and nutrients are often investigated separately in the laboratory, and primarily using a single species, leaving uncertainty about the interactive roles of these environmental variables in driving marine phytoplankton diversity at the community level (Boyd and Hutchins 2012; Boyd et al. 2018).

Both model and empirical studies suggest the temperature–nutrient interaction is substantial. Nutrient availability can inhibit cellular reproduction, shifting the phytoplankton thermal response and altering thermal optima (Thomas et al. 2017). Similarly, temperature can modify cellular metabolism (Eppley 1972), changing the nutrient requirements for growth (Lewington-Pearce et al. 2019). Together, these environmental variables have the potential to act synergistically, changing phytoplankton physiology (Boyd et al. 2016), or unevenly, with one variable emerging as a dominant driver (Brennan and Collins 2015; Qu et al. 2018). These effects may differ among phytoplankton taxa, altering competitive outcomes and shifting community composition (Siegel et al. 2020). Through manipulative experiments, more can be learned about these temperature–nutrient interactions and the mechanisms which drive phytoplankton physiologically and ecologically (Riebesell and Gattuso 2015), both now and in a future ocean (Boyd et al. 2015). Working with natural communities where species are able to interact, makes it possible to observe both direct and indirect effects of these treatments (Boyd et al. 2018), providing ecosystem level insight that cannot as easily be obtained with single-species responses (Gear et al. 2017).

To test whether temperature and nutrient availability can alter phytoplankton community structure, we quantified their individual and interactive effects on the community composition, elemental stoichiometry, and growth of a cold-adapted spring phytoplankton community from Narragansett Bay, Rhode Island. This temperate region is subject to diatom-dominated winter–spring phytoplankton blooms, which have been decreasing in magnitude in recent years, presumed to be due to rising winter water temperatures (Keller et al. 1999), providing a valuable backdrop for our study. We incubated a natural community under an array of thermal and nutrient conditions in order to tease apart the separate and interactive effects of temperature and nutrients on phytoplankton diversity, and quantitatively assess how temperature and nutrients affect size distribution, species composition, and elemental composition of phytoplankton communities.

Methods

Experimental setup

The initial plankton community originated from surface seawater collected on 20 March 2017 from the Narragansett Bay (NBay) Long-term Plankton Time Series site (41.57°N, 71.39°W). The seawater contained a dense phytoplankton community ($9.18 \mu\text{g L}^{-1}$ chlorophyll *a* [Chl *a*]), representative of a moderate spring bloom (Supporting Information Fig. S1). Seawater was filtered through a $200 \mu\text{m}$ mesh to remove macro-zooplankton grazers. At the time of collection, surface temperature and salinity were recorded using a 6920 multi-parameter sonde. At approximately the same time, water was collected from the University of Rhode Island (URI) Graduate School of Oceanography (GSO) aquarium intake, $0.22\text{-}\mu\text{m}$ filtered, and stored for later experimental dilutions. This seawater had a salinity of 30.5, which was similar to in situ conditions (29.3).

Seawater from the time series site was used to set up six incubations at three temperature treatments and two nutrient concentrations (Supporting Information Fig. S2). Incubations were carried out in 2-L polypropylene bottles at either the in situ temperature on the date of collection (2.6°C) or at positive or negative deviations from that temperature (ca. $\pm 3^\circ\text{C}$; -0.5°C and 6°C) in temperature-controlled incubators (I-36LLVL Series, Percival Scientific). This range is characteristic of spring sea surface temperatures in NBay (Supporting Information Fig. S3). Low-temperature incubations began at -1°C , but were adjusted to -0.5°C on Day 2 after some freezing occurred. At each temperature, incubations were set up in triplicate by performing 1 : 1 dilutions of NBay whole surface seawater with either nutrient-amended seawater or nutrient-unamended seawater (controls) using the $0.22\text{-}\mu\text{m}$ filtered seawater from the URI GSO aquarium intake. Nutrient-amended seawater contained f/27.6 concentrations of vitamins and trace metals (Guillard 1975) and final macronutrient concentrations as follows: $32 \mu\text{M}$ nitrate, $32 \mu\text{M}$ silicate, and $2 \mu\text{M}$ phosphate. Controls contained only vitamins and trace metals at f/27.6 concentrations (no macronutrients). Amendments were up to two orders of magnitude greater than in situ concentrations ($0.42 \mu\text{M}$ dissolved inorganic nitrogen, $0.57 \mu\text{M}$ phosphate, $0.30 \mu\text{M}$ silicate), reflecting the upper limits experienced over an annual cycle in NBay (Supporting Information Fig. S3) and allowing for differences to be more easily discerned between treatments.

Incubations were maintained on a 12 : 12 L : D cycle at $115 \mu\text{mol photons m}^{-2} \text{s}^{-1}$ for 10 days to mimic in situ conditions. During that time, growth was monitored with daily in vivo fluorescence measurements using a 10-AU fluorometer (Turner Designs). On Days 3 and 6, incubations were diluted to in situ levels of fluorescence (0.63 Relative Fluorescence Units [RFU]) with nutrient-amended or nutrient-unamended (controls) seawater to replenish nutrient supply, ensuring our replete treatment was nonrate limiting and our control treatment paralleled in situ nutrient concentrations. Due to low

phytoplankton community growth, the control treatments at -0.5°C did not undergo dilutions. At the initiation and conclusion of the experiment, samples were collected for cell enumeration and size-fractionated Chl *a*, and intrinsic growth rates were calculated. Intrinsic growth rates describe phytoplankton growth in the absence of predation and were calculated to assess the direct effects of temperature and nutrients on phytoplankton growth. They were estimated using the two-point dilution method (Morison and Menden-Deuer 2017). Briefly, 2-d incubations were carried out at the conclusion of our experiment at dilutions containing 10% and 100% whole seawater from each treatment. The 10% dilution reduced the potential for predator–prey interactions and allowed for the calculation of the final phytoplankton intrinsic growth rates. In addition, samples were collected for elemental analyses, including biogenic silica (BSi), particulate organic nitrogen (PON), particulate organic carbon (POC), and dissolved nutrients (silicate, nitrate, nitrite, and phosphate).

Phytoplankton community characterization

At the onset and conclusion of the incubation experiments, the microphytoplankton community was identified and quantified to discern treatment effects on community composition. Aliquots from each incubation were fixed in triplicate with 2% acid Lugol's solution for microscopy and 0.1% glutaraldehyde and 2% paraformaldehyde, final concentrations, for flow cytometry. Cell enumeration was conducted by performing cell counts ($\sim > 10\ \mu\text{m}$) on a 1-mL Sedgewick cell-counting chamber (Structure Probe Inc.) using an Eclipse E800 microscope (Nikon). Nanoplankton ($\sim 3\text{--}15\ \mu\text{m}$) and picoplankton ($< 3\ \mu\text{m}$) taxa were then counted using a BD Influx (Becton Dickinson Biosciences) at the Marine Science Research Facility (MSRF) at URI. Only red fluorescent particles (692/40 nm), the size of *Synechococcus* (Forward Scatter > 10 , characterized with orange fluorescence [580/30 nm]) or larger, were counted. SPHERO 3- μm Ultra Rainbow Calibration beads (Spherotech) were used to differentiate between picophytoplankton and nanophytoplankton communities. Flow cytometry data were processed with FlowCal in Python version 3.7.3 (Castillo-Hair et al. 2016). Due to the wealth of data collected, the microzooplankton community was characterized in a separate study (Franzè et al. unpubl.).

Community size structure was also evaluated using size-fractionated chlorophyll. At each dilution time point, whole incubation water was filtered in triplicate onto 25-mm Whatman GF/F filters (GE Healthcare), 5- μm polyester filters, or prefiltered through a 20- μm mesh and then filtered onto 25-mm GF/F filters. This allowed for the calculation of the following size fractions: 0.7–5, 5–20, and $> 20\ \mu\text{m}$. Chlorophyll was then extracted in 90% acetone for 24 h at -20°C . Fluorescence was read on a 10-AU fluorometer (Turner Designs), and data were analyzed according to the techniques described in Graff and Rynearson (2011). The effects of temperature and nutrient concentration on

community size structure, represented by proportion of chlorophyll within each fraction, were evaluated with two-way ANOVAs after testing for normality (Shapiro–Wilk test) and homogeneity (Levene's test).

Ordination and cluster analyses

Analyses of microphytoplankton communities were conducted through a comparison of diversity indices. The relative effects of temperature and nutrient concentration on species composition were assessed using both presence/absence data and microscopy cell counts, allowing for the differentiation of treatment effects on species composition vs. the relative proportions they comprised. Jaccard distance of species presence/absence was utilized to discern dissimilarity between treatments using the SciPy package (Virtanen et al. 2020) in Python. Then, a hierarchical cluster analysis was performed using Ward's method, which minimizes total within cluster variation (Ward 1963). Significance of environmental variables in describing community structure was determined with permutational multivariate ANOVA (PERMANOVA) (Oksanen et al. 2018), after groupings were verified to be homogeneous in dispersion (Anderson 2006; The scikit-bio development team 2020).

Separately, abundance data were evaluated to discern treatment effects on species composition. To begin, species evenness was analyzed with Pielou's metric in the Scikit-bio package (The scikit-bio development team 2020). Then, cell counts were Hellinger transformed to account for the high number of zeroes within the dataset (absent species), lessen the weight given to rare species, and make our ecological data suitable for linear methods (Legendre and Gallagher 2001). A transformation-based redundancy analysis (tb-RDA) was applied to the Hellinger species matrix using the vegan package (Oksanen et al. 2018) in R version 4.0.2. This analysis summarizes the variation in treatment phytoplankton communities in terms of a set of explanatory variables. Here, we constrained the tb-RDA by the treatment variables of temperature (continuous) and nutrient concentration (binary: nutrient amended or nutrient unamended). A *k*-means cluster analysis was then conducted on the Hellinger matrix and results were projected onto the tb-RDA ordination. The optimal number of clusters for this analysis was discerned using the Silhouette method (Rousseeuw 1987). Species shown on the ordination plot were both abundant in incubations and could be explained by at least one axis (cumulative proportion of inertia > 0.4). Figures were constructed using Matplotlib (Hunter 2007) in Python and ggplot (Wickham 2016) in R.

Elemental analyses

At the onset and conclusion of the incubation for all treatments, and additionally at each dilution time point for 2.6°C and 6°C amended treatments, each biological incubation replicate was assessed for POC and PON, and BSi content. POC

and PON were evaluated in triplicate by harvesting cells onto 25-mm GF/F filters which had been precombusted at 450°C for 24 h. Filters were then analyzed on a Costech Elemental Combustion System (Costech Analytical Technologies Inc.). Due to operator error, one replicate had to be discarded from the 6°C amended incubation. BSi content was assessed by filtering cells in triplicate onto 2- μm polycarbonate filters and analyzing them on a Barnstead Turner SP-830 spectrophotometer, following the methods of Strickland and Parsons (1972).

In addition, nutrient analyses of dissolved ammonium, phosphate, silicate, and nitrite/nitrate (total inorganic nitrogen) were evaluated using a Lachat Quikchem 8500 analyzer (Hach) at the MSRF. These elemental measurements allowed for the characterization of total nitrogen and silica in the 2.6°C and 6°C amended treatments over the 10-d incubation.

Results

Community size structure

The proportion of Chl *a* within the > 20 and 5–20 μm size fractions varied significantly between nutrient treatments (Fig. 1; Supporting Information Table S1; two-way ANOVAs). The nutrient-amended treatment was dominated by larger cells, as determined by a greater proportion of chlorophyll in the > 20 μm fraction. Chl *a* size structure did not differ among temperature treatments (Supporting Information Table S1; two-way ANOVAs). However, increasing temperature from –0.5°C to 6.0°C in the presence of replete nutrients increased the biomass of the whole phytoplankton community 3- to 6-fold, as represented by total Chl *a* (Fig. 1; ANOVA, $F[2, 6]$, $p < 0.0001$). These changes in biomass were driven interactively by temperature and nutrient concentration (Supporting Information Table S1; two-way ANOVA, $F = 295.6$, $p < 0.0001$).

Though our phytoplankton communities were dominated by cells > 5 μm (Fig. 1), we also assessed size composition of smaller communities using flow cytometry forward scatter (FSC), a proxy for cell size. Trends in FSC differed from those characterized using Chl *a*, with communities characterized by bimodal size distributions that were significantly different between all treatments (Fig. 2; Mann-Whitney U , $p < 0.0001$), with temperature and nutrients separately, but not interactively, altering size structure (Supporting Information Table S1; two-way ANOVA). FSC was also inversely related to both temperature (Fig. 2A) and nutrient concentration (Fig. 2B; $\text{PCC} = -0.16$ and -0.13 , respectively, $p < 0.0001$), which differed from trends in the total community, where size increased with nutrient availability (Fig. 1). Among the smaller cells, picophytoplankton (< 3 μm) and nanophytoplankton (~ 3–15 μm) abundance were both impacted by the interplay between temperature and resource availability (Supporting Information Table S1, two-way ANOVAs), with picoplankton abundance increasing with temperature (Fig. 2C) in both amended (linear regression: $R^2 = 0.95$, $p = 0.0001$) and unamended treatments ($R^2 = 0.92$, $p = 0.0001$).

Community species composition

During the incubation experiments, phytoplankton communities also underwent compositional rearrangement in response to changes in both temperature and nutrient concentration. The dominant species varied by nutrient treatment. *Leptocylindrus minimus* was most abundant in the unamended treatment community, while *Skeletonema* spp. dominated with nutrient amendments (Fig. 3; Supporting Information Fig. S4). The abundance of *Thalassiosira* spp. also differed by nutrient treatment, with species from this genus present in greater numbers under replete conditions (Supporting Information Table S2; $t[16] = -3.506$, $p = 0.0029$). Some species, such as *Chaetoceros* spp., uncharacterized to species level due mostly

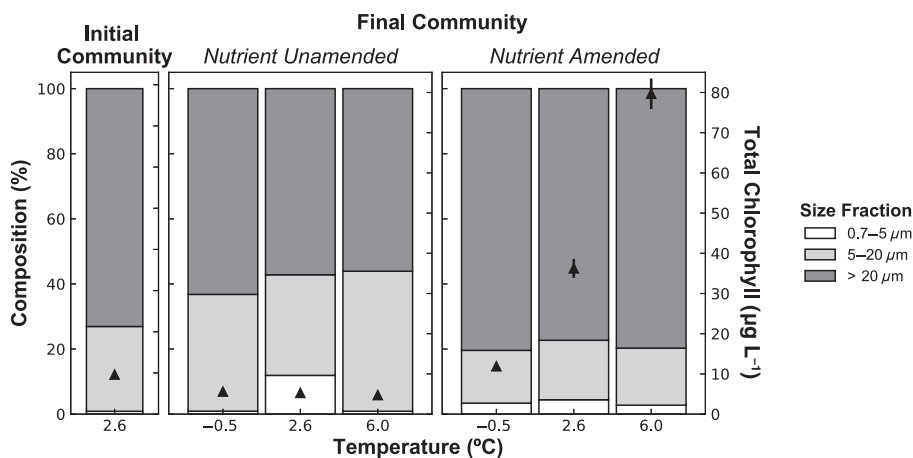


Fig. 1. Community size structure for whole phytoplankton communities. Proportion of Chl *a* from each size fraction is shown from the initial community and after the 10-d incubation (final community) under each nutrient and temperature treatment. Black triangles denote mean total Chl *a* concentration and error bars display the standard deviation of triplicate incubations.

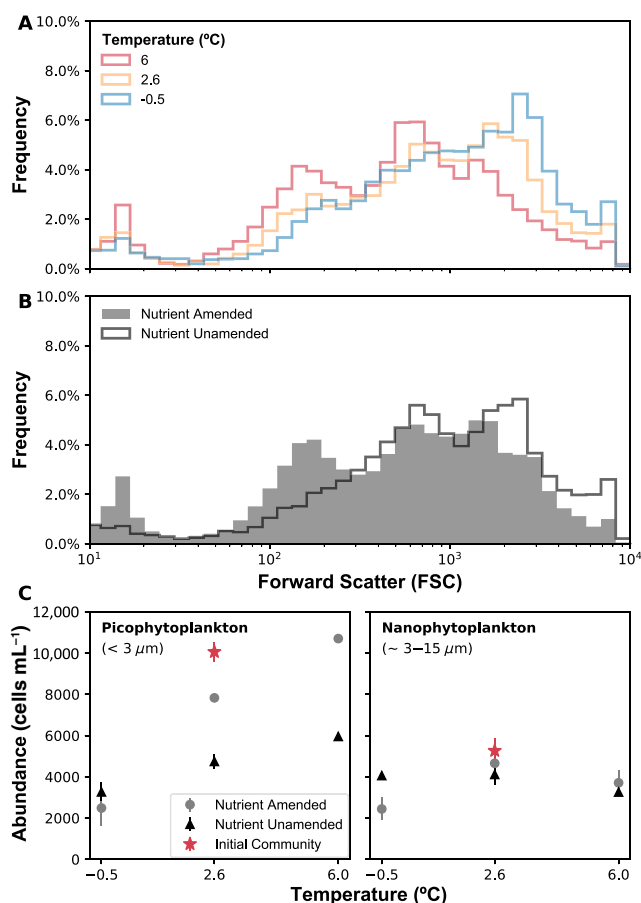


Fig. 2. Size distribution and abundance of phytoplankton communities < 15 μm for all treatments. Forward scatter (FSC), a proxy for cell size, was bimodally distributed and inversely related to both temperature (A) and nutrient concentration (B). Picophytoplankton (< 3 μm) and nanophytoplankton (~ 3–15 μm) cell abundance (C) were both impacted by the interplay between temperature and nutrients. Error bars denote standard deviation in counts between replicates.

to minute size, displayed a clear temperature association, with cell abundance inversely related to temperature (Fig. 3; Supporting Information Fig. S4; $PCC = -0.81$, $p = 0.0083$). In many cases, species abundance scaled with temperature, but the directionality varied by species and nutrient treatment. For instance, *Skeletonema* spp. abundance was positively correlated with temperature in the nutrient-amended treatments ($PCC = 0.97$, $p < 0.0001$) and negatively correlated under the unamended treatments (Fig. 3; Supporting Information Fig. S4; $PCC = -0.89$, $p = 0.0013$).

Species composition under each treatment was evaluated further using presence/absence data. Ward clustering of the Jaccard species matrix resulted in three distinct groups: the initial community, the final nutrient-amended community, and the final nutrient-unamended community (Fig. 4). Nutrients were a significant driver of composition (PERMANOVA, $F = 4.642$, $p = 0.010$), while temperature was not ($F = 1.345$, $p = 0.3$). In addition, the nutrient–temperature interaction was not a significant determinant of the resulting phytoplankton community (PERMANOVA, $F = 0.812$, $p = 0.6$). These results align with our qualitative evaluation of the dominant genera differing between nutrient treatments (Fig. 3).

Temperature–nutrient interaction

Though nutrients were the only significant driver of species composition in our microphytoplankton community, our initial observations that biomass (Fig. 1) and the proportions of specific genera (Fig. 3) scaled with temperature suggested temperature–nutrient interactions may have impacted community composition. We explored this possibility by first examining changes in community intrinsic growth rates (Fig. 5), defined as growth in the absence of grazing. The interactive effect of temperature and nutrient concentration on phytoplankton growth was significant (ANOVA, $F[3,17]$,

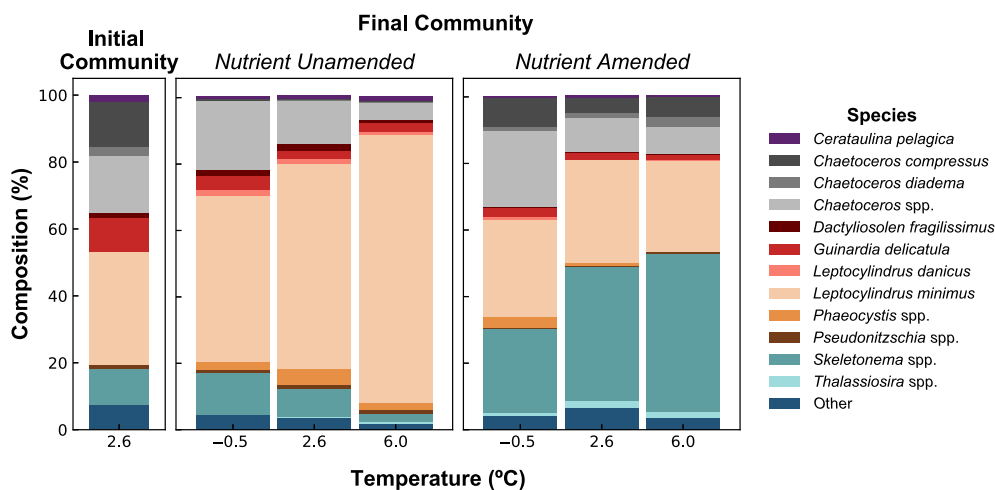


Fig. 3. Community composition discerned via microscopy. Proportions of species representing at least 1% of the community in at least two treatments are shown for the initial community and after the 10-d incubation (final community) under each nutrient regime. All remaining species are pooled and represented as “other.”

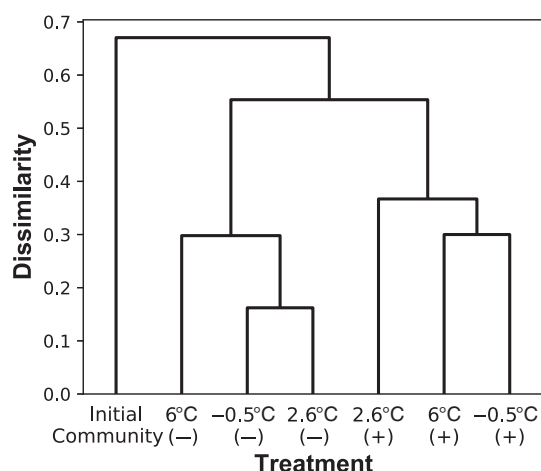


Fig. 4. Community diversity cluster analysis for final phytoplankton communities from incubation experiments. Ward clustering of a Jaccard dissimilarity matrix, utilizing microscopy presence-absence count data, revealed nutrients (+ amended; – unamended) were the primary driver of species composition. Significant groupings included the following: nutrient controls (unamended), nutrient-amended treatments, and the initial community.

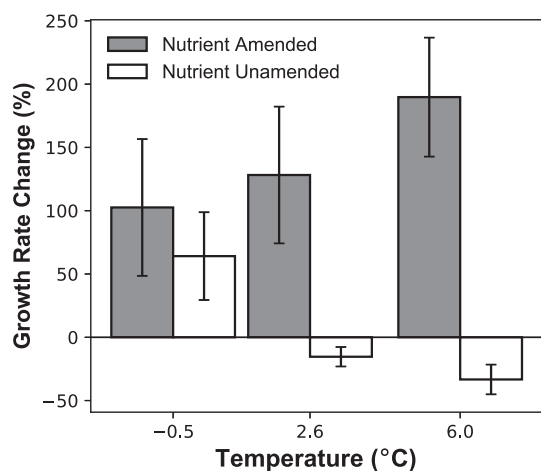


Fig. 5. Percent change in community intrinsic growth rates (growth in the absence of grazing) from experiment onset (Days 0–3) to the final dilution (Days 6–10) for each treatment. Bar height denotes mean percent growth change and error bars display standard deviation for triplicate incubations. Under nutrient-amended conditions, warming is beneficial to phytoplankton growth, while under limited nutrients (unamended), warming adds a secondary stress, reducing growth; together illustrating the complex nature of the temperature–nutrient interaction.

$p = 0.0004$), surpassing the sum effects of temperature and resources individually. When nutrients were plentiful, the temperature–nutrient interaction amplified community growth rates by as much as 189%. However, under nutrient limitation, the temperature–nutrient interaction was antagonistic, depressing growth rates by as much as 33% when compared to that of the initial community (0.13 d^{-1}). Growth

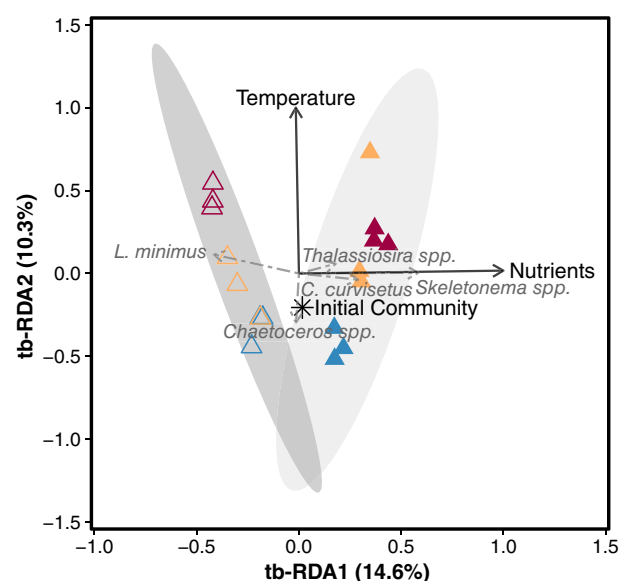


Fig. 6. tb-RDA of final phytoplankton communities assessed via microscopy counts. Points denote community composition for triplicate treatments at -0.5°C (blue), 2.6°C (yellow), and 6°C (red) under nutrient amendments (filled triangles) or in situ nutrient concentrations (open triangles). Star shows initial phytoplankton community and gray ellipses indicate k -means clusters ($n = 2$; Silhouette method). Species of interest are shown in gray. (C.c.: *Chaetoceros curviusetus*; C.spp.: *Chaetoceros* species; L.m.: *Leptocylindrus minimus*; S.spp.: *Skeletonema* species; T.spp.: *Thalassiosira* species).

scaling with temperature and nutrient concentration was not uniform across phytoplankton species. In all treatments, evenness, or the similarity of species proportions between treatments, decreased from that of the initial community, implying treatments acted as selective pressures (Supporting Information Fig. S5). The nutrient-amended treatment was significantly more even than the nutrient control ($t[16] = -3.158$, $p = 0.0061$) and evenness was inversely related to temperature ($\text{PCC} = -0.60$, $p = 0.0065$). However, species richness did not vary to the same extent between treatments (Supporting Information Fig. S6). The initial community had the fewest number of recorded species, implying the resultant community comprised several species that were initially present at concentrations below detection ($< 1 \text{ cell } 40 \text{ mL}^{-1}$).

The temperature–nutrient interaction was explored further with a tb-RDA. This analysis assessed changes in species composition in terms of the treatment variables, temperature, and nutrient concentration (Fig. 6). Treatment communities generally clustered in triplicate, indicating species consistency among biological replicates. The eigenvalues of the first two tb-RDA axes (0.019 and 0.013, respectively) explained 24.94% of the total variance and 57.43% of the constrained variance, indicating that other factors not accounted for in our analysis impacted phytoplankton composition. However, Monte-Carlo permutation revealed temperature and nutrient availability to be significant drivers of this phytoplankton community

($p = 0.025$ and 0.001 , respectively). Our k -means cluster analysis of experimental treatment phytoplankton communities ($k = 2$, Silhouette method) grouped them precisely by nutrient treatment, with the initial community aligning with those from the nutrient-amended treatment. This grouping was consistent with our earlier Ward cluster analysis of species presence/absence, and again signified nutrient availability was the primary factor shaping this phytoplankton community.

Several abundant species were also correlated with the treatment variables in our tb-RDA analysis. For example, *Skeletonema* species and *Chaetoceros compressus* aligned along the nutrient vector (Fig. 6), suggesting they were positively associated with increased nutrient availability, while *Leptocylindrus minimus* excelled when nutrients were relatively limited (Fig. 6). *Chaetoceros* species were inversely related to temperature. *Thalassiosira* species were positively associated with both temperature and nutrient availability. These findings from our tb-RDA analysis are consistent with our earlier qualitative observations of relative genera proportions in the community (Fig. 3) and quantitative assessments of species abundance with nutrient treatments (Supporting Information Table S2), indicating phytoplankton compositional gradients result from a combination of nutrient and thermal responses.

Elemental composition

Changes in community composition resulted in alterations to elemental composition among treatments. While both POC and PON concentrations were expectedly greater under nutrient amendments (Supporting Information Fig. S7), C : N was significantly different among nutrient treatments (Fig. 7A; Supporting Information Table S3; $t[16] = 6.522$, $p < 0.0001$) and displayed opposing trends with temperature depending on nutrient availability. Under limited nutrient availability (unamended), C : N increased with temperature (PCC = 0.80, $p = 0.0092$). This may be due to an increase in carbon storage with temperature (Supporting Information Fig. S7A; Table S3; PCC = 0.87; $p = 0.0022$), while PON stayed constant across temperatures (Supporting Information Fig. S7B; $p = 0.7$). Under replete nutrients, C : N decreased with temperature (PCC = -0.98 , $p < 0.0001$), attributed to a significant increase in nitrogen drawdown with temperature, even when the effects of growth are accounted for (Supporting Information Fig. S8; ANCOVA, $F[2,15]$, $p = 0.0007$). BSi : C was inversely correlated with temperature (Fig. 7B; PCC = -0.42 , $p = 0.0813$), though silica drawdown was not affected by temperature directly (ANCOVA, $F[2,15]$, $p = 0.4$), but rather by community growth rates (PCC = -0.68 , $p = 0.0018$).

Discussion

Several studies have assessed the separate roles of nutrients and temperature in regulating phytoplankton communities. We built upon this existing framework and developed a multivariate study to assess how these individually relevant

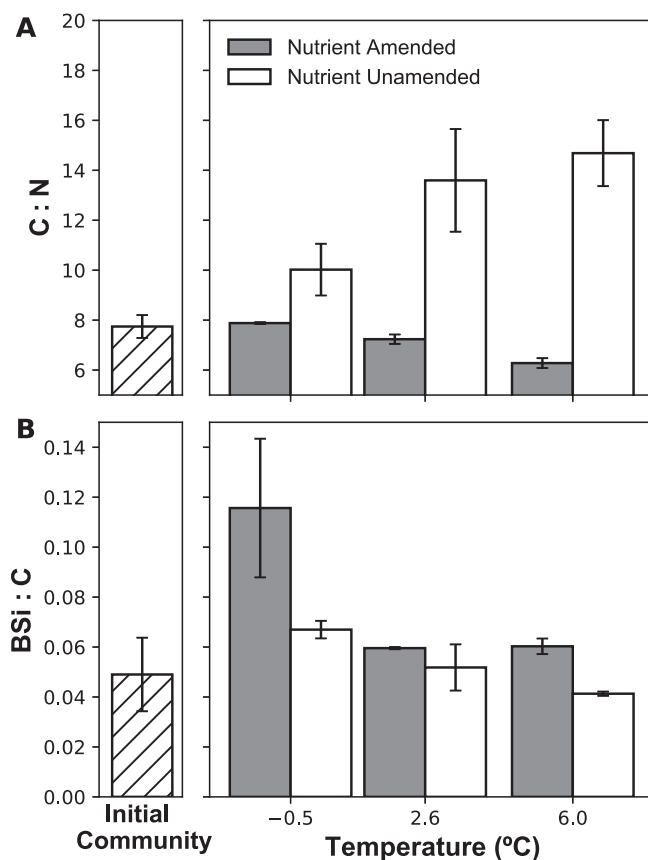


Fig. 7. Whole community final carbon to nitrogen (C : N, **A**) and biogenic silica to carbon (BSi : C, **B**) ratios from the incubation experiments. Left panels show elemental ratios of source water and the error bars denote the standard deviation of biological triplicates.

environmental variables may interact to drive community assembly; addressing a notable gap in the literature (Boyd 2011). We examined how resource competition and environmental filtering might select for species in a community, as they alter species' competitive abilities, highlighting niche and fitness differences (Bestion et al. 2018). These phytoplankton niches, defined by growth, nutrient acquisition, and grazer resistance (Margalef 1978; Litchman et al. 2007), were all under selection in our mesocosm experiments. Resource availability resulted in species sorting, which altered phytoplankton community size composition (Fig. 8). Simultaneously, temperature impacted growth and nutrient drawdown, altering cellular elemental composition. Together, the temperature–nutrient effect shifted the relative proportions of each taxa within the community and altered total phytoplankton biomass.

Our findings of swift community rearrangement, driven interactively by temperature and nutrient concentration, stemmed from a methodology designed to highlight various aspects of community assembly. While many studies measure bulk biomass (chlorophyll), we utilized size-fractionated chlorophyll to

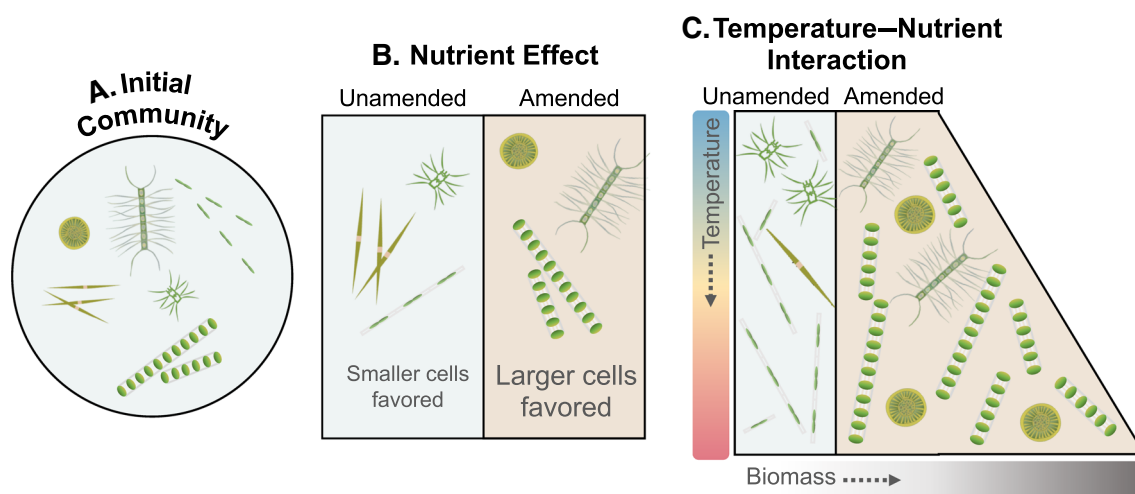


Fig. 8. Summative diagram of the respective roles of temperature and nutrients in structuring a cold-adapted spring phytoplankton community (**A**). Nutrient amendments/limitation resulted in species sorting which modified community size structure (**B**). The temperature response of the communities was strongly dependent on nutrient status with growth rates decreasing when nutrients were limited (unamended) and increasing with nutrient amendments. Together, the temperature-nutrient interaction impacted community biomass, represented by box width, and changed species proportions (**C**). Phytoplankton images courtesy of the Integration and Application Network, University of Maryland Center for Environmental Science (Saxby 2004).

gain a deeper understanding of the community size structure response to changing environmental variables, which have implications for food web dynamics, carbon export, and biogeochemical cycling (Finkel et al. 2010). We also employed microscopy counts to obtain species absolute abundance. While this strategy may not illuminate species richness at the depth of genetic analyses, microscopy is not subject to certain biases like gene copy number, which can vary both between and within species in the plankton (Gong and Marchetti 2019), and alter perceived proportions represented by each species in the community (Gloor et al. 2017). Lastly, by measuring phytoplankton intrinsic growth rates using the dilution method, which minimizes losses due to grazing, we could assess the direct effects of temperature and nutrients on phytoplankton growth. Together, these strategies enabled us to disentangle the relative effects of nutrients and temperature on this phytoplankton community.

Resource availability drives size structure

Nutrient supply is thought to be the principal factor governing phytoplankton size structure (Finkel et al. 2010), with community succession occurring in tandem with nutrient availability (Margalef 1978). Over the course of our incubations, growth decreased with elevated temperature under in situ nutrient concentrations, suggesting communities may have become nutrient limited. This allowed us to place community changes in the context of resource availability, as our spring phytoplankton community shifted in size composition in response to changing nutrient concentrations. For instance, cells $< 20 \mu\text{m}$ were more prevalent when nutrients were limited (unamended), as discerned via Chl *a* concentration. Their greater surface area to volume ratio, smaller diffusive

boundary layer, and lower nutrient requirements needed to attain maximum growth, relative to larger phytoplankton, are thought to explain their greater ability to acquire and utilize surrounding nutrients (Raven 1998). The resulting size structure in these phytoplankton communities may also be attributed to the initial community composition, which was diatom dominated. Diatoms are fast growing opportunists (Litchman et al. 2007), capable of exploiting nutrient pulses more effectively than other phytoplankton within their size class (Cermeno et al. 2011). Due to their larger, armored structures (e.g., spines, frustules), diatoms are also less frequently preyed upon by microzooplankton (Irigoien et al. 2005). Together, these factors may have contributed to the direct nutrient-size relationship observed in our study. Though cell size has a well-characterized inverse relationship with temperature (Atkinson et al. 2003), we only observed a temperature-size relationship in our picophytoplankton and nanophytoplankton communities. This may result from the low resolution captured by our chlorophyll size-fractionations, as opposed to that with flow cytometry, our relatively short incubation period (Helmuth 2009), the relatively small portion of the phytoplankton thermal niche examined, or additional factors not accounted for in our study, such as grazing preferences.

Temperature-nutrient interplay affects community composition

Bottom-up species selection is thought to occur due to resource competition (nutrients) and environmental filtering (temperature) (Vallina et al. 2017), brought about by differences in species' physiological traits which influence their competitive abilities (Bestion et al. 2018). Our results suggest

that this species sorting can occur over a relatively short time scale even when temperature, and therefore metabolic rates, are low. Many of the species that became abundant during the incubation period had previously been found to excel in similar conditions to the ones imposed during our incubations. For example, *Skeletonema* species seem to excel when nutrients, especially silicate (Alves-De-Souza et al. 2008), are available. *Skeletonema* spp.'s inverse relationship with temperature under relatively low nutrient concentrations, suggest for those species, temperature may exacerbate nutrient stress. In contrast, *Leptocylindrus* has been shown to be a strong competitor in low nitrogen regimes (Escaravage et al. 1999). The species *L. minimus* in particular, which was most prevalent in our unamended controls, has a high surface area to volume ratio and has been negatively correlated with nitrate concentration in the field (Alves-De-Souza et al. 2008). Over the weeks following our sampling, *L. minimus* became increasingly prevalent in NBay as temperatures gradually increased to 4.8°C (Supporting Information Fig. S9), suggesting our mesocosms accurately captured natural community dynamics and potentially indicating that NBay became progressively nutrient limited in the weeks following our incubation experiment.

Species proportions were not uniform across treatments, but instead were altered by one or both abiotic variables, as evidenced by their shifting relative abundances within the community. The phytoplankton response to increased temperature and limited nutrient availability lowered community evenness, as a few select genera dominated under the altered environmental conditions. Both temperature and nutrients acted as selective pressures on species composition and altered phytoplankton growth, allowing certain species to propagate over others. Species-energy theory (SET) would predict that the number of species would scale with resource availability (Wright 1983), citing that the probability of stochastic extinction is lessened as biomass increases with nutrient availability (Cardinale et al. 2009). Yet, in our incubations, richness was not correlated with nutrient concentration or biomass. While findings across natural gradients support SET (Lehtinen et al. 2017), observations in manipulation experiments seem to contradict the theory (Suding et al. 2005). This may result from the closed system design of bottle incubations that do not allow for new species immigration. It may also indicate the occurrence of competitive exclusion in our incubations, which SET fails to account for (Vallina et al. 2014).

Though temperature and nutrients were significant drivers of this phytoplankton community, the tb-RDA only explained 24.9% of the total variability within the dataset, suggesting other factors influenced community assembly. These may include biotic interactions, both top-down controls and interspecies competition, which were not accounted for in this study, but are known to occur in tandem with environmental filtering to drive community patterns (Kraft et al. 2015). For example, some microzooplankton grazers within our incubations exhibited prey preferences, which could have influenced

the resulting phytoplankton community (Franzé et al. unpubl.). In addition, one uncharacterized *Chaetoceros* species isolated from the low temperature treatment during our incubation experiment was shown to exhibit a preference for cold, low-light conditions (Kling et al. 2021), suggesting that while we did not alter irradiance, it could be another factor interacting with temperature in this community (Edwards et al. 2016). Thus, final communities may have resulted from a combination of phytoplankton abiotic tolerance to treatment conditions assessed in this study, as well as competitive fitness differences between species (Kraft et al. 2015) and preferential prey selection by microzooplankton grazers (Burkill et al. 1987), which were not excluded by the 200 µm pre-filtration. The microzooplankton grazers within our incubations were also likely affected by the abiotic treatment conditions, as they exhibit varied thermal responses in terms of both growth (Franzé and Menden-Deuer 2020) and grazing (Lawrence and Menden-Deuer 2012).

Altered elemental ratios

Changes in community composition were accompanied by altered elemental ratios. Though cellular carbon and nitrogen content often scale with cell volume (Finkel et al. 2010), they did not do so proportionately in our study. Nutrient replete treatments had C : N ratios close to Redfield proportions (Redfield 1958), but under unamended nutrient conditions, C : N was more than double. This change in C : N resulted from increased carbon storage (Supporting Information Fig. S7A) which may signify a collective community response to nutrient stress (Geider and La Roche 2002). Accumulating carbon allows phytoplankton to more quickly synthesize cellular components once nutrient limitations are alleviated and is a known and effective strategy of the diatoms (Talmy et al. 2014). Disparity in C : N between nutrient treatments may also be attributed to differences in size composition, as smaller phytoplankton, which comprised a greater proportion of the nutrient-unamended community, tend to have lower C : N due to a higher abundance of non-scalable nitrogen containing components, like nucleic acids (Marañón et al. 2013). Trends in BSi : C may similarly reflect differences in community composition, as BSi was proportionately higher at lower temperatures where highly silicified species, like those from the genus *Chaetoceros*, were more prevalent. However, our results, as well as previous studies with the centric diatoms *Thalassiosira pseudonana* and *Coscinodiscus* sp. also suggest cellular silicification may decrease with temperature, independent of taxonomic changes, resulting in thinner frustules at warmer temperatures (Qu et al. 2018; Sheehan et al. 2020).

Conclusion

In this experiment, the temperature-nutrient interaction altered the community dynamics of these cold-adapted phytoplankton. When nutrients were amended, rising temperature

acted as an enhancer, increasing phytoplankton community growth rates and total Chl *a*. When nutrients were unamended, warming acted as a stressor, depressing growth rates and altering species proportions. However, the temperature change examined was not sufficient to impose species selection. While temperature can be a powerful environmental filter (Thomas et al. 2016), the scale of the thermal gradient examined in this experiment did not significantly alter species makeup, suggesting that these phytoplankton were well adapted to the thermal range examined. But because the temperature–nutrient interplay can be either synergistic or antagonistic, considering temperature and nutrients in tandem may prove beneficial when making spatial and temporal projections (Thomas et al. 2017). For example, in the instance of marine heat waves, which are predicted to increase in frequency with climate change (Oliver et al. 2019), assessing the nutrient field in which the heat waves occur could allow for more accurate predictions about the phytoplankton growth response, community size structure, elemental stoichiometry, and potentially even provide some insight regarding the taxa which could proliferate. Each of these factors has implications for trophic dynamics, carbon flux, and biogeochemical cycling (Finkel et al. 2010). Thus, efforts to disentangle the phytoplankton response to multiple stressors and highlight variable interactions, such as this temperature–nutrient interplay, better represent the complex conditions phytoplankton experience in the natural environment.

References

- Alves-De-Souza, C., M. T. González, and J. L. Iriarte. 2008. Functional groups in marine phytoplankton assemblages dominated by diatoms in fjords of southern Chile. *J. Plankton Res.* **30**: 1233–1243. doi:[10.1093/plankt/fbn079](https://doi.org/10.1093/plankt/fbn079)
- Anderson, M. J. 2006. Distance-based tests for homogeneity of multivariate dispersions. *Biometrics* **62**: 245–253. doi:[10.1111/j.1541-0420.2005.00440.x](https://doi.org/10.1111/j.1541-0420.2005.00440.x)
- Anderson, S. I., and T. A. Ryneerson. 2020. Variability approaching the thermal limits can drive diatom community dynamics. *Limnol. Oceanogr.* **65**: 1961–1973. doi:[10.1002/lno.11430](https://doi.org/10.1002/lno.11430)
- Aranguren-Gassis, M., C. T. Kremer, C. A. Klausmeier, and E. Litchman. 2019. Nitrogen limitation inhibits marine diatom adaptation to high temperatures. *Ecol. Lett.* **22**: 1860–1869. doi:[10.1111/ele.13378](https://doi.org/10.1111/ele.13378)
- Atkinson, D., B. J. Ciotti, and D. J. S. Montagnes. 2003. Protists decrease in size linearly with temperature: ca. 2.5% °C. *Proc. R. Soc. B Biol. Sci.* **270**: 2605–2611. doi:[10.1098/rspb.2003.2538](https://doi.org/10.1098/rspb.2003.2538)
- Bestion, E., B. García-Carreras, C. E. Schaum, S. Pawar, and G. Yvon-Durocher. 2018. Metabolic traits predict the effects of warming on phytoplankton competition. *Ecol. Lett.* **21**: 655–664. doi:[10.1111/ele.12932](https://doi.org/10.1111/ele.12932)
- Boyd, P. W. 2011. Beyond ocean acidification. *Nat. Geosci.* **4**: 273–274. doi:[10.1038/ngeo1150](https://doi.org/10.1038/ngeo1150)
- Boyd, P. W. 2019. Physiology and iron modulate diverse responses of diatoms to a warming Southern Ocean. *Nat. Clim. Change* **9**: 148–152. doi:[10.1038/s41558-018-0389-1](https://doi.org/10.1038/s41558-018-0389-1)
- Boyd, P. W., and D. A. Hutchins. 2012. Understanding the responses of ocean biota to a complex matrix of cumulative anthropogenic change. *Mar. Ecol. Prog. Ser.* **470**: 125–135. doi:[10.3354/meps10121](https://doi.org/10.3354/meps10121)
- Boyd, P. W., and others. 2016. Physiological responses of a Southern Ocean diatom to complex future ocean conditions. *Nat. Clim. Change* **6**: 207–213. doi:[10.1038/nclimate2811](https://doi.org/10.1038/nclimate2811)
- Boyd, P. W., S. T. Lennartz, D. M. Glover, and S. C. Doney. 2015. Biological ramifications of climate-change-mediated oceanic multi-stressors. *Nat. Clim. Change* **5**: 71–79. doi:[10.1038/nclimate2441](https://doi.org/10.1038/nclimate2441)
- Boyd, P. W., and others. 2018. Experimental strategies to assess the biological ramifications of multiple drivers of global ocean change—A review. *Glob. Chang. Biol.* **24**: 2239–2261. doi:[10.1111/gcb.14102](https://doi.org/10.1111/gcb.14102)
- Brennan, G., and S. Collins. 2015. Growth responses of a green alga to multiple environmental drivers. *Nat. Clim. Change* **5**: 892–897. doi:[10.1038/nclimate2682](https://doi.org/10.1038/nclimate2682)
- Burkill, P. H., R. F. C. Mantoura, C. A. Llewellyn, and N. J. P. Owens. 1987. Microzooplankton grazing and selectivity of phytoplankton in coastal waters. *Mar. Biol.* **93**: 581–590. doi:[10.1007/BF00392796](https://doi.org/10.1007/BF00392796)
- Cardinale, B. J., H. Hillebrand, W. S. Harpole, K. Gross, and R. Ptacnik. 2009. Separating the influence of resource “availability” from resource “imbalance” on productivity–diversity relationships. *Ecol. Lett.* **12**: 475–487. doi:[10.1111/j.1461-0248.2009.01317.x](https://doi.org/10.1111/j.1461-0248.2009.01317.x)
- Castillo-Hair, S. M., J. T. Sexton, B. P. Landry, E. J. Olson, O. A. Igoshin, and J. J. Tabor. 2016. FlowCal: A user-friendly, open source software tool for automatically converting flow cytometry data from arbitrary to calibrated units. *ACS Synth. Biol.* **5**: 774–780. doi:[10.1021/acssynbio.5b00284](https://doi.org/10.1021/acssynbio.5b00284)
- Cermeño, P., J. B. Lee, K. Wyman, O. Schofield, and P. G. Falkowski. 2011. Competitive dynamics in two species of marine phytoplankton under non-equilibrium conditions. *Mar. Ecol. Prog. Ser.* **429**: 19–28. doi:[10.3354/meps09088](https://doi.org/10.3354/meps09088)
- Doblin, M. A., and E. van Sebille. 2016. Drift in ocean currents impacts intergenerational microbial exposure to temperature. *Proc. Natl. Acad. Sci.* **113**: 5700–5705. doi:[10.1073/pnas.1521093113](https://doi.org/10.1073/pnas.1521093113)
- Edwards, K. F., M. K. Thomas, C. A. Klausmeier, and E. Litchman. 2016. Phytoplankton growth and the interaction of light and temperature: A synthesis at the species and community level. *Limnol. Oceanogr.* **61**: 1232–1244. doi:[10.1002/lno.10282](https://doi.org/10.1002/lno.10282)
- Eppley, R. W. 1972. Temperature and phytoplankton growth in the sea. *Fish. Bull.* **70**: 1063–1085.

- Escaravage, V., T. C. Prins, C. Nijdam, A. C. Smaal, and J. C. H. Peeters. 1999. Response of phytoplankton communities to nitrogen input reduction in mesocosm experiments. *Mar. Ecol. Prog. Ser.* **179**: 187–199. doi:[10.3354/meps179187](https://doi.org/10.3354/meps179187)
- Finkel, Z. V., J. Beardall, K. J. Flynn, A. Quigg, T. A. V. Rees, and J. A. Raven. 2010. Phytoplankton in a changing world: Cell size and elemental stoichiometry. *J. Plankton Res.* **32**: 119–137. doi:[10.1093/plankt/fbp098](https://doi.org/10.1093/plankt/fbp098)
- Franzè, G., and S. Menden-Deuer. 2020. Common temperature–growth dependency and acclimation response in three herbivorous protists. *Mar. Ecol. Prog. Ser.* **634**: 1–13. doi:[10.3354/meps13200](https://doi.org/10.3354/meps13200)
- Geider, R. J., and J. La Roche. 2002. Redfield revisited: Variability of C:N:P in marine microalgae and its biochemical basis. *Eur. J. Phycol.* **37**: 1–17. doi:[10.1017/S0967026201003456](https://doi.org/10.1017/S0967026201003456)
- Gloor, G. B., J. M. Macklaim, V. Pawlowsky-Glahn, and J. J. Egozcue. 2017. Microbiome datasets are compositional: And this is not optional. *Front. Microbiol.* **8**: 1–6. doi:[10.3389/fmicb.2017.02224](https://doi.org/10.3389/fmicb.2017.02224)
- Gong, W., and A. Marchetti. 2019. Estimation of 18S gene copy number in marine eukaryotic plankton using a next-generation sequencing approach. *Front. Mar. Sci.* **6**: 1–5. doi:[10.3389/fmars.2019.00219](https://doi.org/10.3389/fmars.2019.00219)
- Graff, J. R., and T. A. Ryneerson. 2011. Extraction method influences the recovery of phytoplankton pigments from natural assemblages. *Limnol. Oceanogr. Methods* **9**: 129–139. doi:[10.4319/lom.2011.9.129](https://doi.org/10.4319/lom.2011.9.129)
- Grear, J. S., T. A. Ryneerson, A. L. Montalbano, B. Govenar, and S. Menden-Deuer. 2017. pCO₂ effects on species composition and growth of an estuarine phytoplankton community. *Estuar. Coast. Shelf Sci.* **190**: 40–49. doi:[10.1016/j.ecss.2017.03.016](https://doi.org/10.1016/j.ecss.2017.03.016)
- Guillard, R. R. L. 1975. Culture of phytoplankton for feeding marine invertebrates, p. 29–60. *In* W. L. Smith and M. H. Chanley [eds.], *Culture of marine invertebrate animals: Proceedings of the 1st Conference on Culture of Marine Invertebrate Animals* Greenport. Springer US.
- Helmuth, B. 2009. From cells to coastlines: How can we use physiology to forecast the impacts of climate change? *J. Exp. Biol.* **212**: 753–760. doi:[10.1242/jeb.023861](https://doi.org/10.1242/jeb.023861)
- Hunter, J. D. 2007. Matplotlib: A 2D graphics environment. *Comput. Sci. Eng.* **9**: 90–95. doi:[10.1109/MCSE.2007.55](https://doi.org/10.1109/MCSE.2007.55)
- Hutchinson, G. E. 1961. The paradox of the plankton. *Am. Nat.* **95**: 137–145.
- Irigoin, X., K. J. Flynn, and R. P. Harris. 2005. Phytoplankton blooms: A “loophole” in microzooplankton grazing impact? *J. Plankton Res.* **27**: 313–321. doi:[10.1093/plankt/fbi011](https://doi.org/10.1093/plankt/fbi011)
- Keddy, P. A. 1992. Assembly and response rules: Two goals for predictive community ecology. *J. Veg. Sci.* **3**: 157–164. doi:[10.2307/3235676](https://doi.org/10.2307/3235676)
- Keller, A. A., C. A. Oviatt, H. A. Walker, and J. D. Hawk. 1999. Predicted impacts of elevated temperature on the magnitude of the winter–spring phytoplankton bloom in temperate coastal waters: A mesocosm study. *Limnol. Oceanogr.* **44**: 344–356. doi:[10.4319/lo.1999.44.2.0344](https://doi.org/10.4319/lo.1999.44.2.0344)
- Kling, J., K. Kelly, S. Pei, T. Ryneerson, and D. Hutchins. 2021. Irradiance modulates thermal niche in a previously undescribed low-light and cold-adapted nano-diatom. *Limnol. Oceanogr.* **66**(6): 2266–2277. doi:[10.1002/lno.11752](https://doi.org/10.1002/lno.11752)
- Kraft, N. J. B., P. B. Adler, O. Godoy, E. C. James, S. Fuller, and J. M. Levine. 2015. Community assembly, coexistence and the environmental filtering metaphor. *Funct. Ecol.* **29**: 592–599. doi:[10.1111/1365-2435.12345](https://doi.org/10.1111/1365-2435.12345)
- Lawrence, C., and S. Menden-Deuer. 2012. Drivers of protistan grazing pressure: Seasonal signals of plankton community composition and environmental conditions. *Mar. Ecol. Prog. Ser.* **459**: 39–52. doi:[10.3354/meps09771](https://doi.org/10.3354/meps09771)
- Legendre, P., and E. D. Gallagher. 2001. Ecologically meaningful transformations for ordination of species data. *Oecologia* **129**: 271–280. doi:[10.1007/s004420100716](https://doi.org/10.1007/s004420100716)
- Lehtinen, S., T. Tamminen, R. Ptacnik, and T. Andersen. 2017. Phytoplankton species richness, evenness, and production in relation to nutrient availability and imbalance. *Limnol. Oceanogr.* **62**: 1393–1408. doi:[10.1002/lno.10506](https://doi.org/10.1002/lno.10506)
- Lewington-Pearce, L., A. Narwani, M. K. Thomas, C. T. Kremer, H. Vogler, and P. Kratina. 2019. Temperature-dependence of minimum resource requirements alters competitive hierarchies in phytoplankton. *Oikos* **128**: 1194–1205. doi:[10.1111/oik.06060](https://doi.org/10.1111/oik.06060)
- Litchman, E., C. A. Klausmeier, O. M. Schofield, and P. G. Falkowski. 2007. The role of functional traits and trade-offs in structuring phytoplankton communities: Scaling from cellular to ecosystem level. *Ecol. Lett.* **10**: 1170–1181. doi:[10.1111/j.1461-0248.2007.01117.x](https://doi.org/10.1111/j.1461-0248.2007.01117.x)
- Litchman, E., P. de Tezanos Pinto, C. A. Klausmeier, M. K. Thomas, and K. Yoshiyama. 2010. Linking traits to species diversity and community structure in phytoplankton. *Hydrobiologia* **653**: 15–28. doi:[10.1007/s10750-010-0341-5](https://doi.org/10.1007/s10750-010-0341-5)
- Marañón, E., P. Cermeño, D. C. López-Sandoval, T. Rodríguez-Ramos, C. Sobrino, M. Huete-Ortega, J. M. Blanco, and J. Rodríguez. 2013. Unimodal size scaling of phytoplankton growth and the size dependence of nutrient uptake and use. *Ecol. Lett.* **16**: 371–379. doi:[10.1111/ele.12052](https://doi.org/10.1111/ele.12052)
- Margalef, R. 1978. Life-forms of phytoplankton as survival alternatives in an unstable environment. *Oceanol. Acta* **1**: 493–509. <https://archimer.ifremer.fr/doc/00123/23403/>
- Moore, C. M., and others. 2013. Processes and patterns of oceanic nutrient limitation. *Nat. Geosci.* **6**: 701–710. doi:[10.1038/ngeo1765](https://doi.org/10.1038/ngeo1765)
- Morel, F. M. M., and N. M. Price. 2003. The biogeochemical cycles of trace metals in the oceans. *Science* **300**: 944–947. doi:[10.1126/science.1083545](https://doi.org/10.1126/science.1083545)
- Morison, F., and S. Menden-Deuer. 2017. Doing more with less? Balancing sampling resolution and effort in measurements of

- protistan growth and grazing-rates. *Limnol. Oceanogr. Methods* **15**: 794–809. doi:[10.1002/lom3.10200](https://doi.org/10.1002/lom3.10200)
- Oksanen, J., and others. 2018. *vegan*: Community ecology package. R package version 2.5-6. Available from <https://CRAN.R-project.org/package=vegan>
- Oliver, E. C. J., and others. 2019. Projected marine heatwaves in the 21st century and the potential for ecological impact. *Front. Mar. Sci.* **6**: 1–12. doi:[10.3389/fmars.2019.00734](https://doi.org/10.3389/fmars.2019.00734)
- Pearson, D. E., Y. K. Ortega, Ö. Eren, and J. L. Hierro. 2018. Community assembly theory as a framework for biological invasions. *Trends Ecol. Evol.* **33**: 313–325. doi:[10.1016/j.tree.2018.03.002](https://doi.org/10.1016/j.tree.2018.03.002)
- Qu, P., F. Fu, and D. A. Hutchins. 2018. Responses of the large centric diatom *Coscinodiscus* sp. to interactions between warming, elevated CO₂, and nitrate availability. *Limnol. Oceanogr.* **63**: 1407–1424. doi:[10.1002/lno.10781](https://doi.org/10.1002/lno.10781)
- Raven, J. A. 1998. The twelfth Tansley lecture. Small is beautiful: The picophytoplankton. *Funct. Ecol.* **12**: 503–513. doi:[10.1046/j.1365-2435.1998.00233.x](https://doi.org/10.1046/j.1365-2435.1998.00233.x)
- Redfield, A. C. 1958. The biological control of chemical factors in the environment. *Am. Sci.* **46**(3): 205–221.
- Riebesell, U., and J. P. Gattuso. 2015. Lessons learned from ocean acidification research. *Nat. Clim. Change* **5**: 12–14. doi:[10.1038/nclimate2456](https://doi.org/10.1038/nclimate2456)
- Rousseeuw, P. J. 1987. Silhouettes: A graphical aid to the interpretation and validation of cluster analysis. *J. Comput. Appl. Math.* **20**: 53–65. doi:[10.1016/0377-0427\(87\)90125-7](https://doi.org/10.1016/0377-0427(87)90125-7)
- Saxby, T. 2004. Integration and application network. Univ. Maryland Center for Environmental Scienc.
- Sheehan, C. E., K. G. Baker, D. A. Nielsen, and K. Petrou. 2020. Temperatures above thermal optimum reduce cell growth and silica production while increasing cell volume and protein content in the diatom *Thalassiosira pseudonana*. *Hydrobiologia* **6**: 4233–4248. doi:[10.1007/s10750-020-04408-6](https://doi.org/10.1007/s10750-020-04408-6)
- Siegel, P., K. G. Baker, E. Low-Décarie, and R. J. Geider. 2020. High predictability of direct competition between marine diatoms under different temperatures and nutrient states. *Ecol. Evol.* **10**: 7276–7290. doi:[10.1002/ece3.6453](https://doi.org/10.1002/ece3.6453)
- Sterner, R. W., and J. J. Elser. 2002. *Ecological stoichiometry: The biology of elements from molecules to the biosphere*. Princeton Univ. Press.
- Strickland, J. D. H., and T. R. Parsons. 1972. *A practical handbook of seawater analysis*, 2nd ed. Bulletin 167: Fisheries Research Board of Canada. Ottawa, Ontario, Canada.
- Suding, K. N., S. L. Collins, L. Gough, C. Clark, E. E. Cleland, K. L. Gross, D. G. Milchunas, and S. Pennings. 2005. Functional- and abundance-based mechanisms explain diversity loss due to N fertilization. *Proc. Natl. Acad. Sci. USA* **102**: 4387–4392. doi:[10.1073/pnas.0408648102](https://doi.org/10.1073/pnas.0408648102)
- Sunagawa, S., and others. 2015. Structure and function of the global ocean microbiome. *Science* **348**: 1261359. doi:[10.1126/science.1261359](https://doi.org/10.1126/science.1261359)
- Talmy, D., J. Blackford, N. J. Hardman-Mountford, L. Polimene, M. J. Follows, and R. J. Geider. 2014. Flexible C:N ratio enhances metabolism of large phytoplankton when resource supply is intermittent. *Biogeosciences* **11**: 4881–4895. doi:[10.5194/bg-11-4881-2014](https://doi.org/10.5194/bg-11-4881-2014)
- The Scikit-bio Development Team. 2020. *Scikit-bio: A bioinformatics library for data scientists, students, and developers*.
- Thomas, M. K., C. T. Kremer, and E. Litchman. 2016. Environment and evolutionary history determine the global biogeography of phytoplankton temperature traits. *Glob. Ecol. Biogeogr.* **25**: 75–86. doi:[10.1111/geb.12387](https://doi.org/10.1111/geb.12387)
- Thomas, M. K., M. Aranguren-Gassis, C. Kremer, M. R. Gould, K. Anderson, C. A. Klausmeier, and E. Litchman. 2017. Temperature—Nutrient interactions exacerbate sensitivity to warming in phytoplankton. *Glob. Chang. Biol.* **23**: 3269–3280. doi:[10.1111/gcb.13641](https://doi.org/10.1111/gcb.13641)
- Vallina, S. M., M. J. Follows, S. Dutkiewicz, J. M. Montoya, P. Cermenio, and M. Loreau. 2014. Global relationship between phytoplankton diversity and productivity in the ocean. *Nat. Commun.* **5**: 1–10. doi:[10.1038/ncomms5299](https://doi.org/10.1038/ncomms5299)
- Vallina, S. M., P. Cermenio, S. Dutkiewicz, M. Loreau, and J. M. Montoya. 2017. Phytoplankton functional diversity increases ecosystem productivity and stability. *Ecol. Model.* **361**: 184–196. doi:[10.1016/j.ecolmodel.2017.06.020](https://doi.org/10.1016/j.ecolmodel.2017.06.020)
- Virtanen, P., and others. 2020. SciPy 1.0: Fundamental algorithms for scientific computing in Python. *Nat. Methods* **17**: 261–272. doi:[10.1038/s41592-019-0686-2](https://doi.org/10.1038/s41592-019-0686-2)
- Ward, J. H. J. 1963. Hierarchical grouping to optimize an objective function. *J. Am. Stat. Assoc.* **58**: 236–244. doi:[10.1080/01621459.1963.10500845](https://doi.org/10.1080/01621459.1963.10500845)
- Wickham, H. 2016. *ggplot2: Elegant graphics for data analysis*. Springer-Verlag.
- Wright, D. H. 1983. Species-energy theory: An extension of species-area theory. *Oikos* **41**: 496–506.

Acknowledgments

This research was supported by a NSF Dimensions of Diversity award to T.A.R. (OCE-1638834), E.L. (OCE-1638958), and D.A.H. (OCE-1638804) as well as OCE-1736635 to S.M.-D., and OIA-1655221 to the University of Rhode Island. Support for T.A.R. was also provided by the URI Coastal Institute. We thank the captain of the Cap'n Bert research vessel for sampling assistance. Part of this research was conducted using the University of Rhode Island's Marine Science Research Facility and the seawater facilities at the Ann Gull Durbin Marine Research Aquarium, which are supported by NSF EPSCoR awards OIA-1004057 and OIA-1655221.

Conflict of interest

None declared.

Submitted 02 June 2021

Revised 15 October 2021

Accepted 12 December 2021

Associate editor: Birte Matthiessen